Ultrafast Energy Migration in Platinum(II) Diimine Complexes Bearing Pyrenylacetylide Chromophores

Evgeny O. Danilov,[‡] Irina E. Pomestchenko,[†] Solen Kinayyigit,[†] Pier L. Gentili,[§] Muriel Hissler,[||,⊥] Raymond Ziessel,[||] and Felix N. Castellano*[,†]

Department of Chemistry and Center for Photochemical Sciences, Bowling Green State University, Bowling Green, Ohio 43403, Ohio Laboratory for Kinetic Spectrometry, Bowling Green State University, Bowling Green, Ohio 43403, Laboratoire de Chimie Moléculaire, ECPM, 25 rue Becquerel, 67087 Strasbourg Cedex 02, France, and Laboratoire Organométallique et Catalyse: Chimie et Electrochimie Moléculaires, CNRS-Université de Rennes 1, Institut de Chimie de Rennes 1, Campus de Beaulieu, F-35042 Rennes, France

Received: October 15, 2004; In Final Form: December 15, 2004

The ultrafast excited-state dynamics of three structurally related platinum(II) complexes has been investigated using femtosecond transient absorption spectrometry in 2-methyltetrahydrofuran (MTHF). Previous work has shown that Pt(dbbpy)(C≡C−Ph)$_2$ (dbbpy is 4,4′-di(*tert*-butyl)-2,2′-bipyridine and C≡C−Ph is ethynylbenzene) has a lowest metal-to-ligand charge transfer (^{3}MLCT) excited state, while the multichromophoric Pt(dbbpy)-(C≡C−pyrene)$_2$ (C≡C−pyrene is 1-ethynylpyrene) contains the MLCT state, but possesses a lowest intraligand (^{3}IL) excited state localized on one of the C≡C−pyrenyl units (Pomestchenko, I. E.; Luman, C. R.; Hissler, M.; Ziessel, R.; Castellano, F. N. *Inorg. Chem.* **2003**, *42*, 1394−96). *trans*-Pt(PBu$_3$)$_2$(C≡C−pyrene)$_2$ serves as a model system that provides a good representation of the C≡C−pyrene-localized ^{3}IL state in a Pt(II) complex lacking the MLCT excited state. Following 400 nm excitation, the formation of the ^{3}MLCT excited state in Pt(dbbpy)(C≡C−Ph)$_2$ is complete within 200 ± 40 fs, and intersystem crossing to the ^{3}IL excited state in *trans*-Pt(PBu$_3$)$_2$(C≡C-pyrene)$_2$ occurs with a time constant of 5.4 ± 0.2 ps. Selective excitation into the low-energy MLCT bands in Pt(dbbpy)(C≡C−pyrene)$_2$ (λ_{ex} = 480 nm) leads to the formation of the ^{3}IL excited state in 240 ± 40 fs, suggesting ultrafast wire-like energy migration in this molecule. The kinetic data suggest that the presence of the MLCT states in Pt(dbbpy)(C≡C−pyrene)$_2$ markedly accelerates the formation of the triplet state of the pendant pyrenylacetylide ligand. In essence, the triplet sensitization process is kinetically faster than pure intersystem crossing in *trans*-Pt(PBu$_3$)$_2$(C≡C−pyrene)$_2$ as well as vibrational relaxation in the MLCT excited state of Pt(dbbpy)(C≡C−Ph)$_2$. These results are potentially important for the design of chromophores intended to reach their lowest excited state on subpicosecond time scales and advocate the likelihood of wire-like behavior in triplet−triplet energy transfer.

Introduction

The coupling of transition metals or transition metal complexes with selected organic chromophores has generated new molecules and materials that exhibit a wide range of fundamentally interesting and potentially useful excited-state properties. Square planar platinum(II) complexes and oligomeric materials bearing acetylide units have demonstrated promise in wide-ranging applications including optical power limiting,[1,2] electroluminescence,[3] singlet oxygen photosensitizers,[4] multielectron-transfer processes,[5] and as extrinsic luminescent probes.[6] One interesting category of these molecules is platinum(II) diimine complexes bearing acetylide ligands.[3,7−17] In general, these molecules are highly luminescent, and the lowest energy absorption bands can be attributed to Pt → diimine metal-to-ligand charge-transfer (MLCT) transitions. In most instances, the $^3\pi-\pi^*$ states associated with the acetylide or the diimine substituents are so high in energy that the excited-state behavior is completely dictated by decay of the ^{3}MLCT level, yielding charge-transfer-based luminescence. However, if the $^3\pi-\pi^*$ states associated with the acetylide units are strategically placed below the ^{3}MLCT level, then the charge-transfer states can be used to internally sensitize the production of one of the triplet arylaceylide moieties located trans to the diimine system.[3,15−17] With the aid of the internal heavy atom, long lifetime room-temperature phosphorescence can ensue. Our group,[15,16,18] the Schanze group,[17] and the Che group[3] all have illustrative examples of this excited-state behavior.

While the number of Pt(II) diimine bis(arylacetylide) chromophores are expanding, their subnanosecond excited-state dynamics remain completely unexplored, with the exception of one study by McGarrah and Eisenberg involving the detection of charge-separated products in donor−acceptor dyads at initial delay times of 100 ps following a 20 ps laser pulse.[13] Because the acetylide linkages are expected to provide strong "wire-like" electronic contact to the Pt(II) center,[19,20] we became interested in the excited-state evolution of the ^{3}MLCT state as

* To whom correspondence should be addressed. E-mail: castell@bgnet.bgsu.edu.
† Department of Chemistry and Center for Photochemical Sciences, Bowling Green State University.
‡ Ohio Laboratory for Kinetic Spectrometry, Bowling Green State University.
§ Visiting research scholar from the Department of Chemistry, Perugia University, Perugia, Italy.
|| Laboratoire de Chimie Moléculaire.
⊥ CNRS-Université de Rennes 1.

10.1021/jp045269+ CCC: $30.25
Published on Web 03/01/2005

well as its subsequent depopulation resulting from potentially strong interactions with arylacetylide-localized ^{3}IL states. In a recent contribution, we have demonstrated that low-energy Pt → dbbpy MLCT transitions in Pt(dbbpy)(C≡C−pyrene)$_2$ (**1**) (dbbpy is 4,4′-di(*tert*-butyl)-2,2′-bipyridine and C≡C-pyrene is 1-ethynylpyrene) can be used to internally sensitize the production of the $^3\pi-\pi^*$ excited state localized on one of the pyrenylacetylide moieties trans to the diimine system.[15] Note that the design of **1** places the $^3\pi-\pi^*$ state energy significantly below the ^{3}MLCT* state; therefore, the photophysics is completely dominated by the former. Room-temperature phosphorescence is easily observed from the localized $^3\pi-\pi^*$ state, facilitated by the internal heavy atom. This molecule has a strong triplet-to-triplet absorption centered near 530 nm, which decays by first-order kinetics to the ground state. Therefore, transient absorption measurements can be used to directly track the production of the ligand-localized triplet state in this molecule.

The current work expands on our previous supra-nanosecond study by applying ultrafast transient absorption measurements to this multichromophoric system to measure the time constant of the triplet sensitization process. The two model compounds investigated are Pt(dbbpy)(C≡C−Ph)$_2$ (**2**) (C≡C−Ph is ethynylbenzene) and *trans*-Pt(PBu$_3$)$_2$(C≡C−pyrene)$_2$ (**3**). The former serves as a structural model possessing a low-lying MLCT excited state, whereas the latter provides a good representation of the C≡C−pyrene-localized ^{3}IL state in a Pt(II) complex lacking the MLCT excited state. The ultrafast dynamics of these complexes were investigated in MTHF using 400 nm (all three compounds) and 480 nm excitation (compound **1** only). After 400 nm excitation, the formation of the ^{3}MLCT excited state in **2** is complete within 200 ± 40 fs and intersystem crossing to the ^{3}IL excited state in **3** occurs within 5.4 ± 0.2 ps. Selective excitation into the low-energy MLCT bands in **1** (λ_{ex} = 480 nm) leads to the rapid formation of the ^{3}IL excited state in 240 ± 40 fs, significantly faster than intersystem crossing in the model complex, indicative of ultrafast energy migration in this molecule.

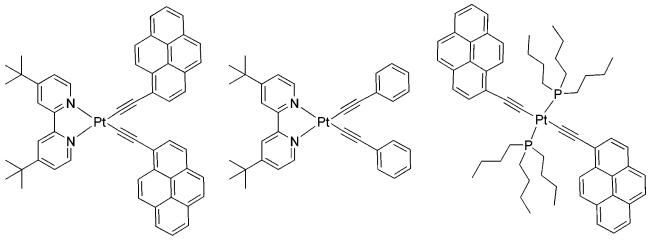

1 **2** **3**

Experimental Section

General. All compounds used in this study were available from our previous work.[15] The primary spectroscopic solvent 2-methyltetrahydrofuran (MTHF, 99$^+$%) was purchased from Acros and used without further purification. Static absorption spectra were measured on a HP 8453 diode array spectrometer. Steady-state photoluminescence spectra were obtained with an Edinburgh Instruments single photon counting spectrofluorimeter (FL/FS 900). Nanosecond laser flash photolysis experiments were performed as described previously.[16] In some instances, sample excitation was afforded by pumping a H_2-filled Raman shifter with the YAG third harmonic to yield 416 nm laser pulses (2−3 mJ/pulse). All spectroscopic measurements were conducted at ambient temperature, 22 ± 2 °C.

Ultrafast Transient Absorption Spectrometry. Femtosecond time-resolved experiments were performed using the spectrometer available in the Ohio Laboratory for Kinetic Spectrometry at BGSU. The output of the laser system consists of pulses of 800 nm, 1 mJ, 100 fs (fwhm) operating at a repetition rate of 1 kHz. The Hurricane output is first split (85% and 15%) into pump and probe beams. The pump beam is converted to selected excitation wavelengths by coupling it into a second-harmonic generator (for 400 nm excitation) or into an optical parametric amplifier (Spectra-Physics OPA 800C, for tunable wavelengths in the region 320−700 nm). The probe beam is first passed through a computer-controlled delay line (Newport Corp. MTL 250 PP 1 250 mm linear positioning stage) that provides an experimental time window of about 1.6 ns with a step resolution of 6.6 fs. After the delay line, the laser beam is focused onto a 3 mm thick sapphire plate that generates a white light continuum (effective useful range, 450−750 nm). The pump beam is passed through an optical chopper (DigiRad C-980) rotating at a frequency of 100 Hz, and focused to a spot size of ∼0.7 mm onto the sample cell. The white light continuum probe beam is collimated and focused into the sample cell, superimposed on the pump beam at an angle of approximately 5°. The energy of the probe pulses was <5 μJ at the sample. After passing through the sample cell, the probe continuum is coupled into a 400 μm optical fiber connected to a CCD spectrograph (Ocean Optics, PC 2000). The delay line and the CCD spectrograph are computer-controlled by a LabVIEW (National Instruments) software routine developed by Ultrafast Systems, LLC (Bowling Green, OH). The samples are continuously flowed during the course of the experiments in an optical cell with a path length of 2 mm (Quartz flow cell, Starna Cells). The sample solutions were prepared to have an absorbance between 0.5 and 1.0 at the excitation wavelength in the 2 mm flow cell. The absorption spectra of the solutions measured before and after each experiment showed no significant sample decomposition in the MTHF solvent. We note that in freshly distilled CH_2Cl_2, significant sample decomposition occurred in some instances, obviating the use of MTHF.

Results and Discussion

Absorption and Photoluminescence Properties. The photophysical properties of **1**−**3** have been examined in CH_2Cl_2, and these results are reported in a previous contribution.[15] Because ultrafast experiments performed in freshly distilled CH_2Cl_2 yielded permanent photochemical decomposition products in some instances, MTHF was selected as the spectroscopic solvent. Figure 1a displays the absorption spectra of **1**−**3** measured in MTHF. The pyrenylacetylide chromophores in **1** are largely responsible for the structured $\pi-\pi^*$ transitions between 350 and 400 nm. These absorptions are substantially red-shifted relative to the uncoordinated pyrene−C≡C−H species,[15] suggesting large σ-donation of the −C≡C−pyrenyl electron density to the Pt(II) center. The visible absorption bands near 450 nm are assigned to dπ Pt→π^* dbbpy MLCT transitions and, although red-shifted, are qualitatively similar to **2**. The MLCT assignment is consistent with the negative solvatochromic shifts observed for the low-energy absorption bands in **1** and **2**.[11,13,16] The higher energy ligand-localized $\pi-\pi^*$ transitions between 350 and 400 nm resulting from electronic transitions within the pyrenylacetylide fragments in **1** are not significantly perturbed by solvent polarity.[15] Similar results are obtained for the structural model **3**, suggesting that the low-energy pyrenyl-based $\pi-\pi^*$ transitions are truly ligand-localized and do not exhibit appreciable charge-transfer character.

The RT emission spectrum of **2** was easily measured in aerated MTHF, whereas the corresponding spectrum for **1** is

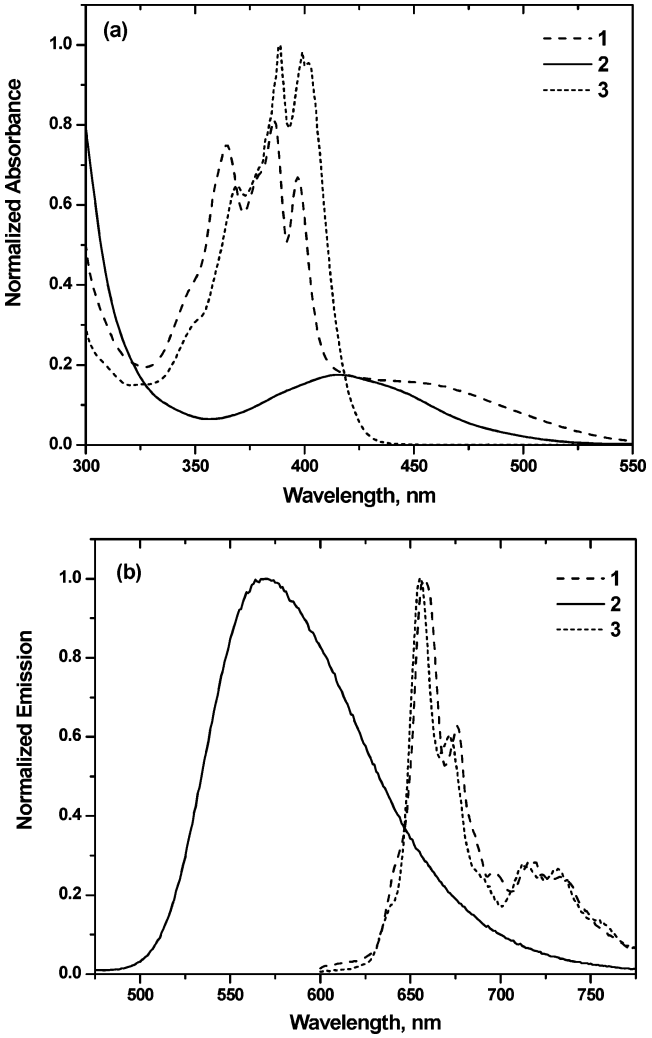

Figure 1. Normalized absorption (a) and photoluminescence (b) spectra for **1**−**3** in deaerated MTHF at room temperature. The emission spectra were measured using 400 ± 2 nm excitation.

nearly quantitatively quenched by dioxygen, necessitating its removal, Figure 1b. Excitation at 400 nm produces a distinct emission spectrum in each case. The luminescence in **2** has already been shown to originate from a MLCT manifold,[7,11,12,16] whereas the emission from **1** is red-shifted (over 100 nm), structured, and relatively sharp by comparison and almost quantitatively matches the room-temperature phosphorescence exhibited by structural model compound **3**, Figure 1b. In the cases of **1** and **3**, the emissions are most consistent with ^{3}IL phosphorescence emanating from a pyrenylacetylide moiety. Our previous work has shown that selective excitation of the low-energy MLCT transitions in **1** (λ_{ex} = 480 nm) sensitizes the production of the ^{3}IL pyrenylacetylide-based phosphorescence in CH_2Cl_2 (λ_{max} = 659 ± 2 nm).[15] Not surprising, the results obtained in MTHF are essentially identical in emission maximum (658 ± 2 nm) and spectral profile, illustrating that the minor modification in solvent polarity does not affect the nature of the lowest ^{3}IL excited state.

Nanosecond Transient Absorption Spectroscopy. Figure 2a displays the excited-state absorption difference spectrum obtained for model complex **2** in MTHF recorded at several delay times after a 416 nm laser pulse. This spectrum is representative of the "relaxed" ^{3}MLCT excited state. Our current laser flash photolysis system cannot adequately suppress the charge-transfer emission above 500 nm, so difference spectra were not recorded at longer wavelengths for **2**. However, the

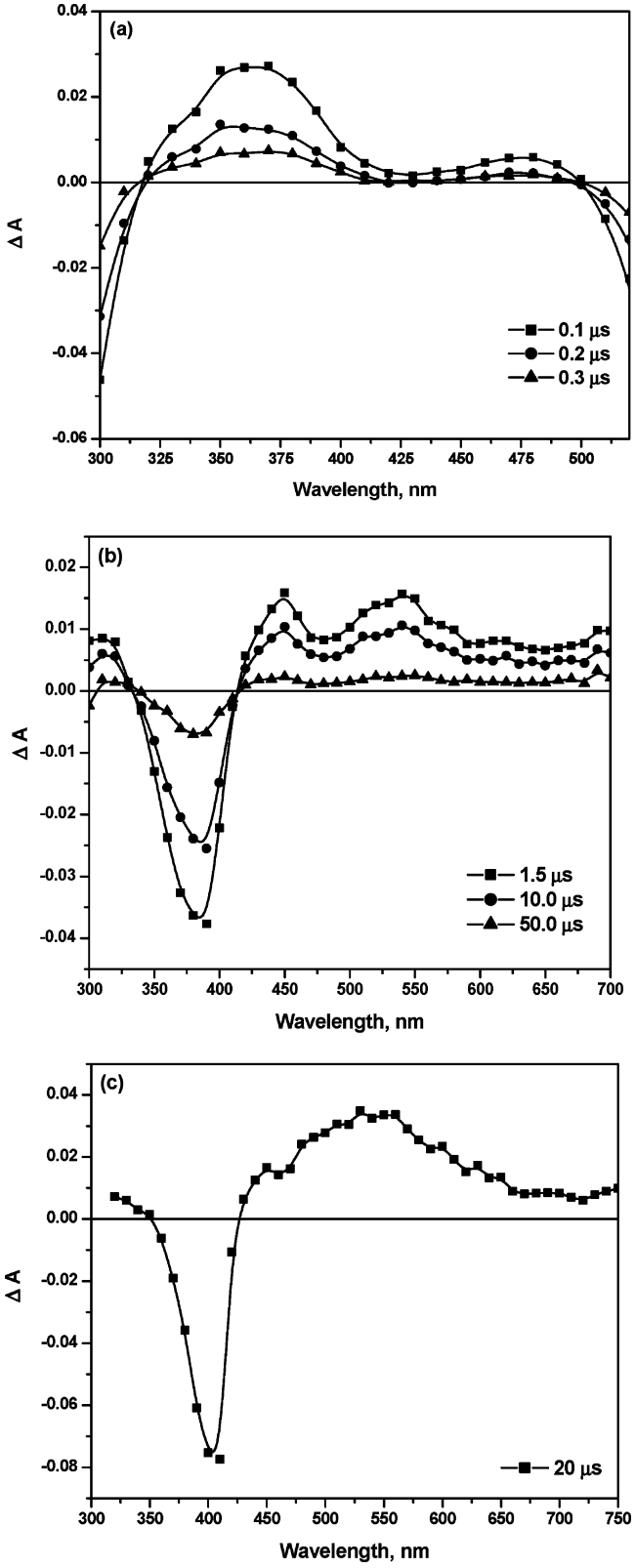

Figure 2. Nanosecond excited-state absorption spectra of **2** (a), **1** (b), and **3** (c) measured at the specified delay times. Spectra a and b were acquired following 416 nm excitation in deaerated MTHF, while spectrum c was measured with 355 nm excitation in deaerated CH_2Cl_2.

recent literature reports the excited-state absorption difference spectra of Pt(dbbpy)(C≡C−PhCH$_3$)$_2$ (measured with an ICCD system) which is structurally identical to **2** with the minor exception of an extra methyl group appended to each phenylacetylide.[12] We therefore expect the excited-state spectra of both

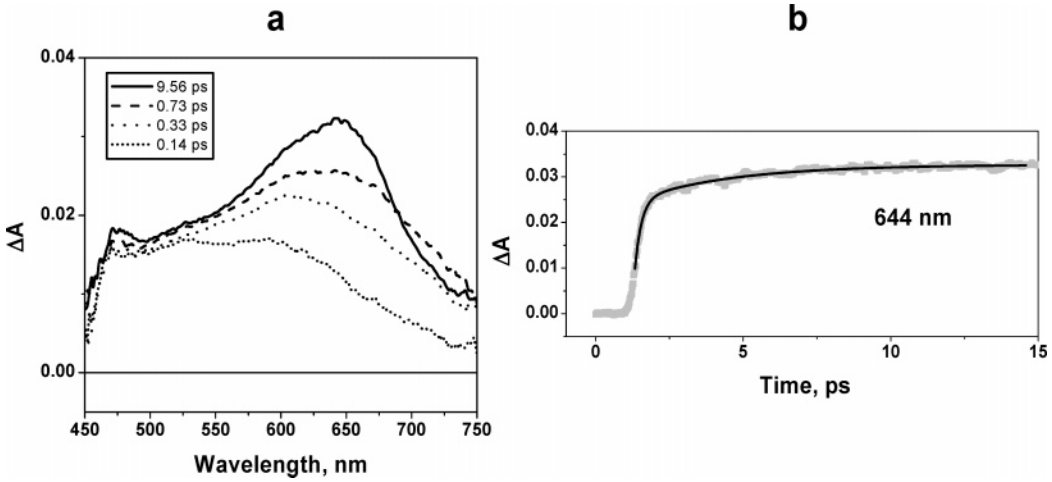

Figure 3. Transient absorption spectra of compound **2** in MTHF following the 100 fs 400 nm excitation pulse (a); the kinetic trace at 644 nm with the biexponential solid line fit superimposed with time constants of 200 fs and 3.6 ps (b).

species to be nearly identical, and Pt(dbbpy)(C≡C−$PhCH_3$)$_2$ displays UV and blue transient absorption features similar to those found in **2**. In addition, Pt(dbbpy)(C≡C−$PhCH_3$)$_2$ possesses a broad long wavelength transient centered around 680 nm, so we would expect an analogous spectroscopic signature for **2**. Although this long wavelength feature can be attributed to the ^{3}MLCT excited state, it is not likely associated with the reduced dbbpy ligand as there are no significant long wavelength absorptions in this moiety as deduced from reductive spectroelectrochemistry experiments.[9] Because this spectroscopic feature is much too strong to result from a d−d transition, it is most likely due to a ligand-to-metal charge-transfer (LMCT) transition. In any case, this transition of uncertain origin is most definitely associated with the "relaxed" ^{3}MLCT excited state and is expected to be observed in the ultrafast measurements, where the MLCT luminescence will be suppressed.

The excited-state absorption difference spectrum of **1** (λ_{ex} = 416 nm) measured in MTHF at a variety of delay times is displayed in Figure 2b. As fast as can be resolved with the nanosecond instrument (~7 ns), a broad absorption transient is observed in the visible ($\lambda_{max} \approx$ 450 and 540 nm) along with ground-state bleaching at higher energy (~380 nm). These spectral features are nearly identical to the difference spectrum previously measured in CH_2Cl_2.[15] The position of the ground-state bleaching maximum corresponds to the highest intensity vibronic ground-state absorption band of the appended −C≡C−pyrene units. By inference to our other data, we interpret this observation as resulting from triplet state sensitization, which in turn bleaches the pyrene-localized ground-state absorption. This transient spectrum decays away with first-order kinetics, $\tau = 25\ \mu$s, in quantitative agreement with time-resolved photoluminescence measurements performed under the same conditions (τ = 24 μs). This indicates that the excited-state species independently detected with luminescence and transient absorption are most likely of the same origin. Because ultrafast measurements consumed our entire stock of **3**, we could not perform nanosecond transient absorption experiments on this compound in MTHF. However, previous flash photolysis measurements performed on **3** following 355 nm excitation in CH_2Cl_2 (Figure 2c) are adequate for comparative purposes because the band positions of the "relaxed" ligand-localized excited state are not expected to be significantly solvent dependent. If necessary, ultrafast difference measurements taken at long delay times can also be used to represent the relaxed ^{3}IL excited state in MTHF.

Femtosecond Transient Absorption Spectroscopy. The ultrafast excited-state difference spectra measured for **2** in MTHF (λ_{ex} = 400 nm) are collected in Figure 3 and focus on the long-wavelength region of the spectrum, which is limited by our sapphire continuum generation. The time evolution of this spectrum echoes the interpretations put forth in describing the ultrafast behavior of $[Ru(bpy)_3]^{2+}$ and related Ru(II) complexes.[21−24] Within 200 fs, the broad transient absorption between 500 and 750 nm associated with the ^{3}MLCT excited state ($\lambda_{max} \approx$ 665 nm) is largely formed. This feature narrows down with time (λ_{max} = 640 nm) and increases in intensity until roughly 10 ps after the laser pulse. The kinetics of this process is also evaluated in Figure 3, corresponding to a 644 nm probe wavelength following 400 nm excitation. The data are adequately fit to a sum of single exponentials. Because only first-order kinetic processes are expected after the impulse response, all ultrafast data are fit using multiexponential functions when adequate single exponential fits are not possible. At the probe wavelength of 644 nm, the MLCT formation process was adequately modeled using a biexponential function, with a fast component that is 200 fs and a longer component of 3.6 ps. The blue-shifting of the red-side of this absorption band hallmarks vibrational relaxation presumably occurring on the ^{3}MLCT surface,[23] and no further spectral shifts are resolved at longer delay times. In essence, the difference spectrum measured after 10 ps is similar to the spectrum measured in the nanosecond experiments, demonstrating that the thermalized ^{3}MLCT excited state is attained in ~10 ps after 100 fs laser excitation at 400 nm. At the present time, we cannot offer a definitive explanation of why the apparent vibrational relaxation in **2** is slower than in $[Ru(bpy)_3]^{2+}$. However, we note that there are significant differences in their molecular structures, ligand fields, charge-transfer energy gaps, and nonradiative decay modes. Based upon these substantial variations, one would not necessarily expect similar excited-state dynamics.

The dynamic absorption processes occurring in model complex **3** are displayed in Figure 4. In this case, 400 nm excitation directly produces the lowest singlet excited state of the C≡C−pyrenyl chromophore. Immediately following the laser pulse, an intense absorption transient with a peak near 630 nm is observed. This is attributed to an excited-state absorption of the singlet state. As time elapses, this feature decays away and another transient feature between 500 and 550 nm appears. The emerging band at higher energy is consistent with that observed for the triplet-to-triplet absorption of the

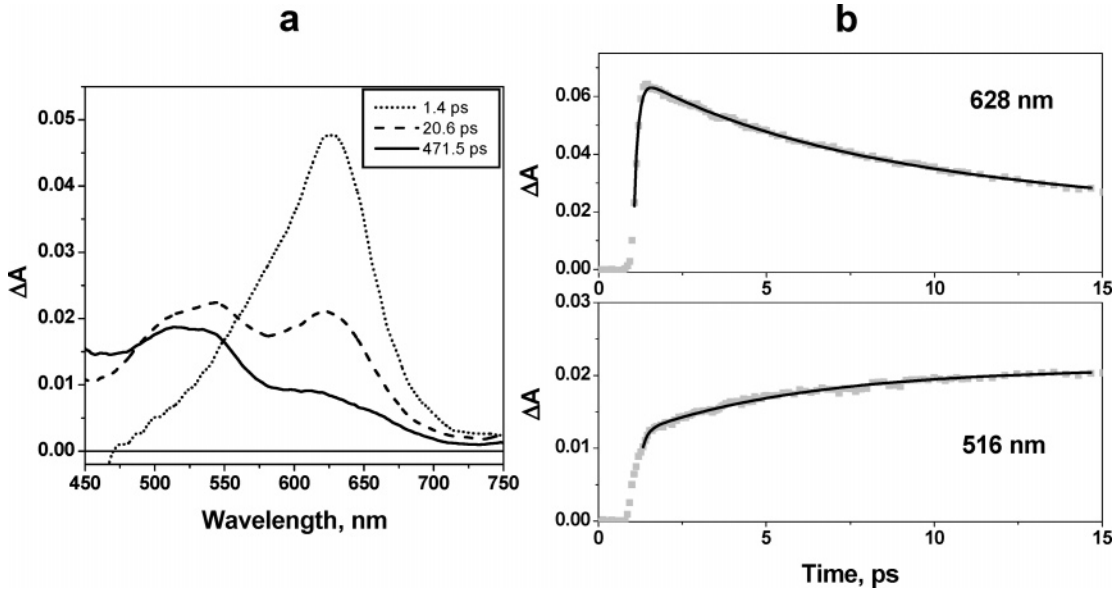

Figure 4. Transient absorption spectra of compound **3** in MTHF measured at three different delay times following a 100 fs, 400 nm excitation pulse (a); the kinetic traces at 628 and 516 nm with their multiexponential solid line fits superimposed (b). In the upper panel of (b), three time constants were required to adequately fit the rise (t = 149 fs) and decay (t = 5.56 and 23.6 ps) simultaneously. The long component is not physically significant and is required only as an "infinitely long" kinetic feature to facilitate the fitting. In the lower panel of (b), two time constants were required to fit the kinetic growth, an instrument-limited time constant of 131 fs and a second time constant of 5.19 ps.

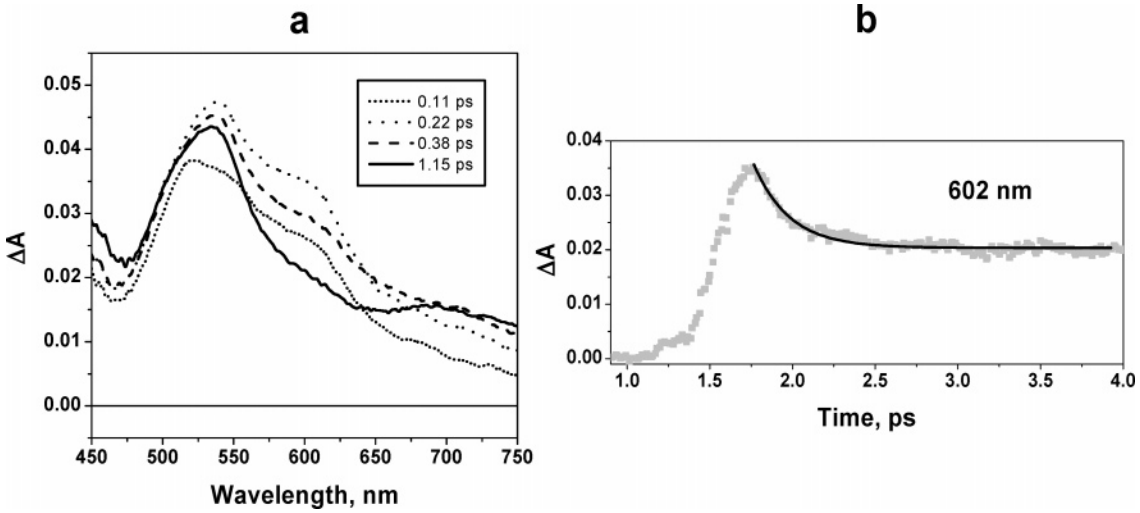

Figure 5. Transient absorption spectra of compound **1** in MTHF at several delay times following a 100 fs, 400 nm excitation pulse (a); the absorption transient at 602 nm along with its corresponding solid line single-exponential fit (τ = 210 fs) superimposed (b).

appended C≡C−pyrenyl unit measured by laser flash photolysis on the microseconds time scale, Figure 2c. The disappearance of the band at 628 nm along with the formation of the band between 500 and 550 nm directly yields the time constant of intersystem crossing, which varies from 5.2 to 5.6 ps, Figure 4. This range was established from independent multiexponential fits of several single probe wavelengths. For brevity, representative data obtained at 628 and 516 nm (along with their multiexponential fits) are displayed in Figure 4b.

While the spectroscopic assignments of the model systems are relatively straightforward, the transient data obtained for **1** do not appear to be simply a superposition of the relaxed excited states that are observed in **2** and **3**. In addition, the transient features associated with the MLCT excited state in **1** may not precisely resemble the MLCT excited state measured in **2**. This simply results from the fact that the ground-state spectra are substantially different and therefore associated LMCT transitions in the MLCT excited state will likely reflect this difference. In any case, we investigated the ultrafast dynamics in **1** at two distinct pump wavelengths, 400 and 480 nm. The former was selected to uniformly correlate time constants because this wavelength was used to pump both model compounds. The 400 nm excitation indiscriminately pumps both the MLCT and the IL singlet states in **1**, producing an ill-defined excited-state composition, making it difficult to track sequential progression of the excitation energy, Figure 5. As can be ascertained by simple inspection of the spectra, the one feature that is genuinely present at all delay times can be attributed to the ^{3}C≡C−pyrene excited state (500−550 nm), which indicates that the triplet sensitization process is substantially fast. Some of the features at long wavelengths may indicate the presence of the ^{1}C≡C−pyrene excited state as well as the ^{3}MLCT excited state, but the substantial overlap of these bands and the lack of isosbestic points render clear-cut assignments virtually impossible. The time evolution of the single wavelength kinetics indicates an instrument-limited growth process followed by a rapid decay of 210 fs, which reduces the transient absorption intensity by about one-half at 602 nm (Figure 5b). After this time, no further

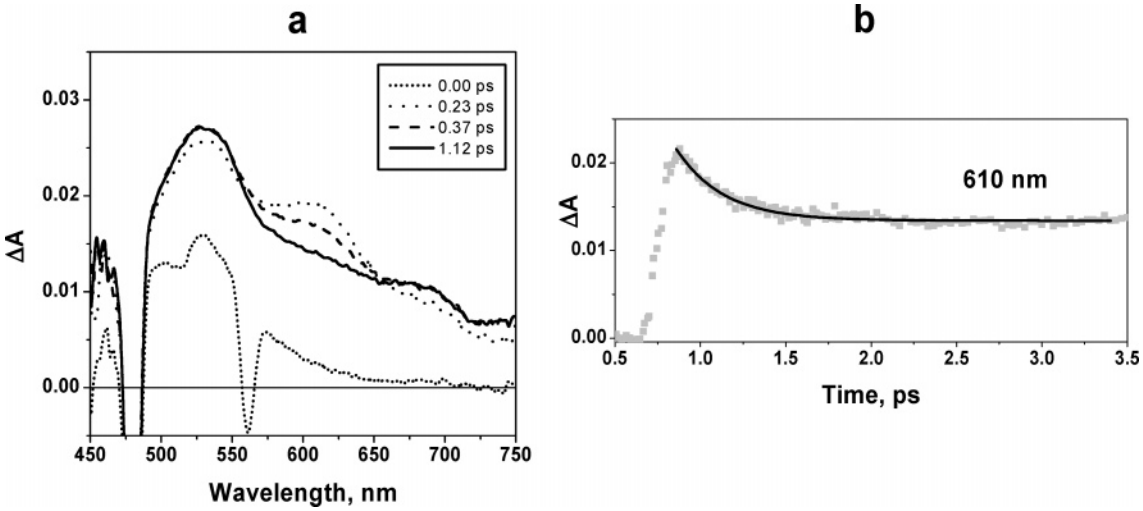

Figure 6. Transient absorption spectra of compound **1** in MTHF at several delay times following a 100 fs, 480 nm excitation pulse (a); the absorption transient at 610 nm along with its corresponding single exponential ($\tau = 240$ fs) solid fit line superimposed (b).

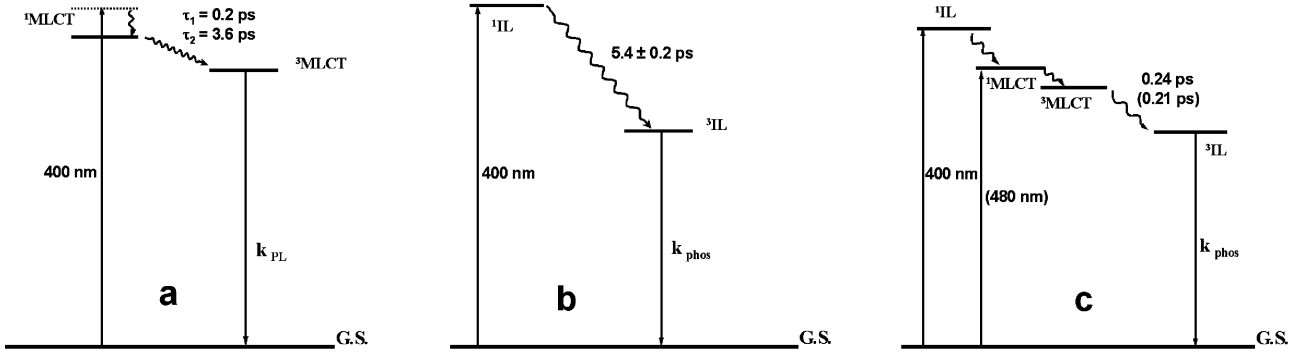

Figure 7. Qualitative energy level diagrams for compounds **2** (a), **3** (b), and **1** (c) summarizing the ultrafast time constants measured in this study (k_{phos} indicates radiative decay through phosphorescence; k_{PL} indicates radiative photoluminescence decay). Nonradiative decay from each lowest excited state also occurs but is purposely not indicated.

changes in the spectrum are observed on the ultrafast time scale. We believe this indicates the process of either the ^{1}C≡C−pyrene excited state or the ^{3}MLCT excited state converting into the ^{3}C≡C−pyrene excited state. Particularly noteworthy is the fact that the indiscriminate excitation and subsequent kinetic processes lead to the production of the lowest triplet state in **1** at a rate that is more than an order of magnitude faster than the pure intersystem crossing process measured in model complex **3**.

Selective excitation of the low-energy MLCT transition in **1** ($\lambda_{ex} = 480$ nm) yields essentially identical kinetics and absorption transients relative to the 400 nm pump experiments, Figure 6. At all delay times, it is clear that the transient feature near 540 nm is present, while the absorption at 610 nm partially decays away with a time constant of 240 fs after its prompt instrument-limited formation. Because the feature at 610 nm contains contributions from both the MLCT excited state and the ^{3}IL state, the decay process is attributed to the depletion of the charge-transfer excited state (Figure 6b). Therefore, we conclude that the time constant of the formation of the ^{3}IL state in **1** is 240 fs, following 480 nm excitation. Because the differences in the triplet sensitization time constants measured at 400 and 480 nm are only 30 fs (210 vs 240 fs), these processes can be considered kinetically identical under our current experimental conditions. The data measured at both pump wavelengths suggest that the presence of the MLCT manifold enables the rapid sensitization of the ligand-localized ^{3}C≡C−pyrene excited state in **1**. The magnitude of the time constants suggests that there is significant electronic mixing of Pt^{II}, dbbpy, and pyrenylacetylide-based orbitals, which facilitates swift energy migration in this structure. This energy movement occurs at rates which exceed that of direct intersystem crossing in **3** as well as vibrational cooling of the MLCT excited state in **2**. All of the relevant kinetic processes of each molecule are summarized in modified Jablonski diagrams presented in Figure 7. The rapid ultrafast energy transfer kinetics relative to other competitive processes is reminiscent of the noteworthy observations made by Monat and McCusker in an Fe^{II} polypyridyl complex.[25] In their system, MLCT excitation of the low-spin complex resulted in the production of the high spin (formally $\Delta S = 2$) metal-centered ligand-field state in 80 fs. Their result illustrates that the kinetics of intimately linked processes can greatly exceed that of vibrational cooling, which indeed appears to be the case for triplet energy migration in the current study.

Conclusion

This manuscript describes an ultrafast transient absorption study of Pt^{II} complexes possessing MLCT and/or ^{3}IL excited states. In the complex possessing a lowest MLCT excited state (**2**), we have successfully evaluated the dynamics of the charge-transfer excited state, identifying the time scales for its formation as well as its vibrational cooling. In the case of the model system lacking low-lying MLCT excited states (**3**), picosecond intersystem crossing dynamics have been quantified. The complex at the heart of the study (**1**), bearing both MLCT and ^{3}IL excited states, was evaluated using both 400 and 480 nm pump wavelengths. The ^{3}IL excited state is formed with 210−240 fs,

suggesting that the presence of the MLCT manifold enables rapid triplet sensitization in this structure and demonstrates how fast energy can migrate in highly electronically coupled structures. These results warrant further ultrafast spectroscopic investigations of related Pt^{II}-containing metal−organic systems.

Acknowledgment. This work was supported by the National Science Foundation (CAREER Award CHE-0134782 to F.N.C.) and the American Chemical Society (ACS-PRF 36156-G6 to F.N.C.). The Ohio Laboratory for Kinetic Spectrometry, under the direction of Prof. M. A. J. Rodgers, was established and funded by the State of Ohio through the Hayes Investment Fund and the Ohio Board of Regents.

References and Notes

(1) McKay, T. J.; Bolger, J. A.; Staromlynska, J.; Davy, J. R. *J. Chem. Phys.* **1998**, *108*, 5537.

(2) Sun, W.; Wu, Z.-X.; Yang, Q.-Z.; Wu, L.-Z.; Tung, C.-H. *Appl. Phys. Lett.* **2003**, *82*, 850.

(3) Chan, S.-C.; Chan, M. C. W.; Wang, Y.; Che, C.-M.; Cheung, K.-K.; Zhu, N. *Chem.-Eur. J.* **2001**, *7*, 4180.

(4) Zhang, D.; Wu, L.-Z.; Yang, Q.-Z.; Li, X.-H.; Zhang, L.-P.; Tung, C.-H. *Org. Lett.* **2003**, *5*, 3221.

(5) Jude, H.; Krause Bauer, J. A.; Connick, W. B. *J. Am. Chem. Soc.* **2003**, *125*, 3446.

(6) Wong, K. M.-C.; Tang, W.-S.; Chu, B. W.-K.; Zhu, N.; Yam, V. W.-W. *Organometallics* **2004**, *23*, 3459.

(7) Chan, C.-W.; Cheng, L.-K.; Che, C.-M. *Coord. Chem. Rev.* **1994**, *132*, 87.

(8) James, S. L.; Younus, M.; Raithby, P. R.; Lewis, J. *J. Organomet. Chem.* **1997**, *543*, 233.

(9) Adams, C. J.; James, S. L.; Liu, X.; Raithby, P. R.; Yellowless, L. J. *J. Chem. Soc., Dalton Trans.* **2000**, 63.

(10) Connick, W. B.; Geiger, D.; Eisenberg, R. *Inorg. Chem.* **1999**, *38*, 3264.

(11) Hissler, M.; Connick, W. B.; Geiger, D. K.; McGarrah, J. E.; Lipa, D.; Lachicotte, R. J.; Eisenberg, R. *Inorg. Chem.* **2000**, *39*, 447.

(12) Whittle, C. E.; Weinstein, J. A.; George, M. W.; Schanze, K. S. *Inorg. Chem.* **2001**, *40*, 4053.

(13) McGarrah, J. E.; Eisenberg, R. *Inorg. Chem.* **2003**, *42*, 4355.

(14) Wadas, T. J.; Lachicotte, R. J.; Eisenberg, R. *Inorg. Chem.* **2003**, *42*, 3772.

(15) Pomestchenko, I. E.; Luman, C. R.; Hissler, M.; Ziessel, R.; Castellano, F. N. *Inorg. Chem.* **2003**, *42*, 1394.

(16) Pomestchenko, I. E.; Castellano, F. N. *J. Phys. Chem. A* **2004**, *108*, 3485.

(17) Haskins-Glusac, K.; Ghiviriga, I.; Abboud, K. A.; Schanze, K. S. *J. Phys. Chem. B* **2004**, *108*, 4969.

(18) Pomestchenko, I. E. Doctoral Dissertation, Bowling Green State University, 2004.

(19) Rogers, J. E.; Cooper, T. M.; Fleitz, P. A.; Glass, D. J.; McLean, D. G. *J. Phys. Chem. A* **2002**, *106*, 10108.

(20) Liu, Y.; Jiang, S.; Glusac, K.; Powell, D. H.; Anderson, D. F.; Schanze, K. S. *J. Am. Chem. Soc.* **2002**, *124*, 12421.

(21) Damrauer, N. H.; Cerullo, G.; Yeh, A.; Boussie, T. R.; Shank, C. V.; McCusker, J. K. *Science* **1997**, *275*, 54.

(22) Yeh, A. T.; Shank, C. V.; McCusker, J. K. *Science* **2000**, *289*, 935.

(23) McCusker, J. K. *Acc. Chem. Res.* **2003**, *36*, 876.

(24) Bhasikuttan, A. C.; Suzuki, M.; Nakashima, S.; Okada, T. *J. Am. Chem. Soc.* **2002**, *124*, 8398.

(25) Monat, J. E.; McCusker, J. K. *J. Am. Chem. Soc.* **2000**, *122*, 4092.